ESTIMATION OF THE TOTAL LIFE IN FRETTING FATIGUE WITH SPHERICAL CONTACT

Carlos Navarro, Jaime Domínguez

Dpto. de Ingeniería Mecánica y de los Materiales
ESI de Sevilla, Avda. de los Descubrimientos s/n, 41092 Sevilla

ABSTRACT

This paper proposes a method for estimating the total fatigue life in fretting fatigue. It compares the fatigue life of some specimens obtained in a series of fretting fatigue tests with the estimates of total fatigue life using a model that separately takes into account the initiation and propagation of the crack. These fatigue tests were conducted on an aluminum alloy (Al 7075-T6) and the contact pads used were spherical. A discussion is carried out regarding the results to decide the relative importance of the initiation and propagation phases, the model that should be used for short cracks growth analysis and the multiaxial fatigue criteria to be used for the initiation of the crack.

INTRODUCTION

Fretting is a phenomenon that can be observed everyday in service in many mechanical systems elements such as riveted and bolted joints, shrink-fitted couplings, metal ropes and cables, etc. [1]. It appears in systems where service loads cause relative displacement of very small amplitude between contact surfaces. This generates friction forces that add to the load normal to the contact surface and the bulk load of the system. When these forces vary cyclically, cracks initiate and propagate by fatigue mechanisms and this is usually referred to as fretting fatigue.

An important issue in the design of mechanical systems that suffer fretting fatigue is the prediction of the endurance under the design loads and many efforts and resources are dedicated to it. This is a difficult problem and there are different approaches that are aimed at solving it.

There is a general agreement that the fretting fatigue process has two different phases: the fatigue crack initiation and crack propagation, which are due to different mechanisms. Some methods to estimate the fretting fatigue life are based on the initiation mechanism, and use the data obtained in tests with smooth specimens under completely reversed loading, combined with various multiaxial fatigue criteria. This method gives better results when the initiation phase dominates over propagation. Another approach is to use linear elastic fracture mechanics. In this case the initiation life is supposed to be small compared to propagation [2]. Another method is to combine initiation with propagation using a fixed crack initiation length [3].

This paper uses a different method, which combines initiation and propagation defining a non-arbitrary crack initiation length, to estimate the life obtained in a series of fretting fatigue tests.

EXPERIMENTAL DATA

The experimental data were obtained from Wittkowsky [4]. The material used in the tests was Al 7075-T6 and its main mechanical properties are listed in Table 1. The spherical surfaces and plane specimens were machined from extruded bars with a diameter of 25.4 and 12.7 mm, respectively. Specimens were flat-sided plates with a rectangular gage section and the radius of the spherical pads was 25.4 mm. The grain size perpendicular to the surface was approximately 60 μm.

TABLE 1

MECHANICAL PROPERTIES

UTS **MPa**	**$\sigma_{y0.2}$** **MPa**	**E** **GPa**	**Fatigue strength (Axial load; R= -1) Mpa** 10^6 **cycles**	10^7 **cycles**	10^8 **cycles**	**ΔK_{th} (R= 0)** **MPa $m^{-1/2}$**
572	503	72	214	175	140	2.2

The loads applied in each test are listed in Table 2 and the test setup is shown in Figure 1, where the load *Q* and *P*, which gives rise to the bulk stress σ, are cyclic loads that vary in phase, while *N* is a constant load. This test setup for fretting fatigue is further explained in [5].

TABLE 2

LOADS IN THE FRETTING TESTS

Test	**T1**	**T2**	**T3**	**T4**	**T5**	**T6**	**T7**
N **(N)**	30	20.8	15.6	18.5	16	13.9	8.33
Q **(N)**	15	15	15	13.6	11.7	10	8
σ (Mpa)	85	83	85	77	83	83	83
N_f (cycles)	480000	449500	395000	551000	530000	803000	616500

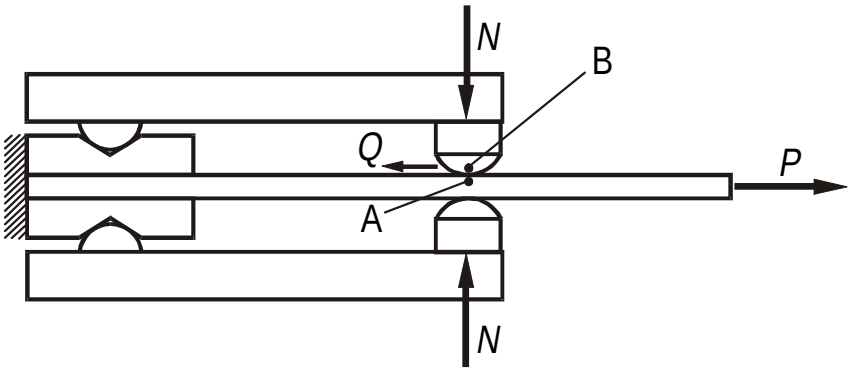

Figure 1: Fretting test loads

INITIATION-PROPAGATION MODEL

The method used in this paper is a modification of Socie, Morrow and Chen [6] for fatigue life analysis of notched members. This modification takes into account the multiaxial characteristics of the stresses produced in a three dimensional contact (spherical contact) instead of a two dimensional contact. They calculated a damage rate caused by crack initiation mechanisms from low cycle fatigue concepts and the damage rate during the crack propagation phase from fracture mechanics concepts. Close to the surface the

damage rate due to crack initiation is higher but at a certain depth the two curves cross. According to their proposal, this point sets the crack initiation length, and below that point the damage rate due to crack propagation exceeds the rate due to initiation mechanisms. The first part is the crack initiation life, N_i, and the second part the crack propagation life, N_p.

In this paper, instead of calculating the damage rates as explained, a similar but numerically equivalent method is used [7]. Along the hypothetical crack path, the fatigue life at each point based on low cycle fatigue is calculated, N_i. This would be the number of cycles needed to initiate a crack at that point. Also, for each point, the number of cycles needed to grow a crack from that point to the final crack, N_p, are calculated using LEFM. The sum of N_i and N_p gives the total life associated to each point. The life of the specimen would be the minimum of that curve, as shown in Figure 2 for the test T3. This point also defines the crack initiation length.

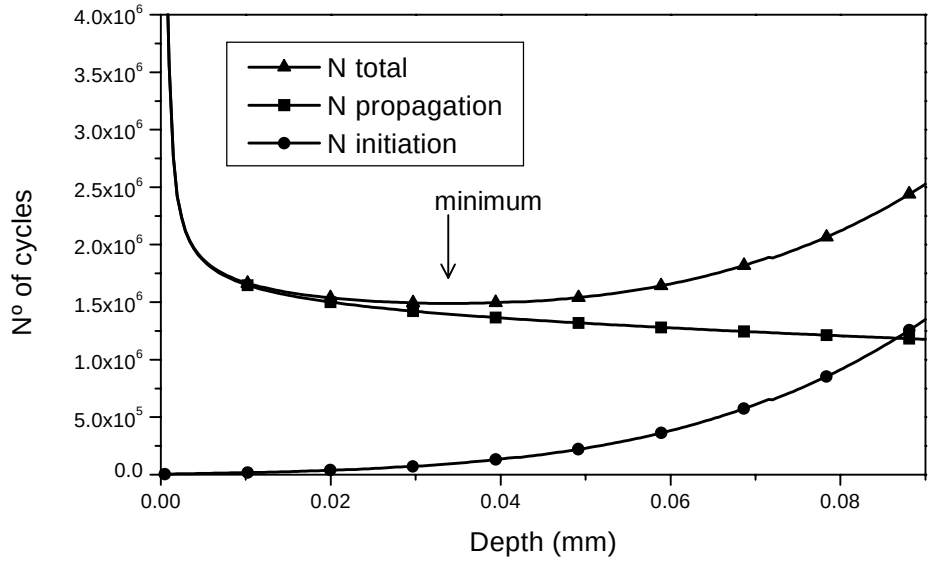

Figure 2: Initiation, propagation and total life estimates for test T9

The stresses produced by spherical contact are calculated analytically using the explicit expressions obtained by Hamilton [8]. Additionally, the eccentricity of the stick zone due to the bulk stress is taken into account as shown in [9]. The first step in order to apply this method is to localize the site of the initiation of the crack. In the tests the cracks initiate at points located very close to the edge of the contact zone. Different multiaxial stress criteria applied at the surface and along the axis of symmetry of the contact zone show that the critical point is the edge of the contact zone, so this point will be chosen for the calculations. The cracks start to grow at a small angle to the surface, but at a depth of about 20 μm they rotate to an angle of 70º-80º. In the application of this method the crack will be supposed to grow perpendicular to the surface. In order to calculate the initiation curve, McDiarmid multiaxial fatigue criterion, Eqn. 1, will be applied [10], together with the strain-life relationship given by Eqn. 2.

$$\frac{\Delta\tau_{max}}{2} + \frac{t}{2\sigma_{TS}}\sigma_{max} = \sigma_{eq} \tag{1}$$

where $\Delta\tau_{max}$ is the maximum increment of tangential stresses, σ_{max} is the maximum normal stress in the direction perpendicular the plane where $\Delta\tau$ is maximum ($\Delta\tau_{max}$), t is the fatigue limit in torsion and σ_{TS} is the ultimate stress.

$$\frac{\Delta\varepsilon}{2} = \frac{\sigma'_f}{E}(2N_i)^b + \varepsilon'_f\,(2N_i)^c \tag{2}$$

where $\Delta\varepsilon$ is the normal strain obtained in tests with smooth specimens under completely reversed loading, E is the Young modulus, N_i are the number of cycles to the initiation of a crack and the rest of the constants depend on the material. In order to combine both equations, it is considered that the stresses are in the elastic regime and the equivalent stress given by McDiarmid is modified by a factor f to be able to introduce it in Eqn. 2. This factor, given in Eqn. 3, is calculated applying McDiarmid criterion in a test with a smooth specimen under completely reversed loading. Therefore, the deformation, $\Delta\varepsilon$, introduced in Eqn. 2 is shown in Eqn. 4.

$$f = \frac{2}{1 + \frac{t}{2\sigma_{TS}}} \tag{3}$$

$$\frac{\Delta\varepsilon}{2} = \frac{\sigma_{eq} \cdot f}{E} \tag{4}$$

The values for the constants are taken from [11], $\sigma'_f = 1917\ MPa \quad b = -0.176 \quad \varepsilon'_f = 0.8 \quad c = -0.839$ for the material Al 7075-T6. The application of this criterion to cracks growing perpendicular to the surface and from points close to the edge of the contact zone give initiation curves that are similar but give higher values of the initiation life when compared to the crack located exactly on the edge. This implies that, supposing the crack grows perpendicular to the surface, the most critical crack is still at the edge of the contact zone.

As it was said earlier, the crack initiates at a small angle and then rotates to an angle of 70º-80º at a depth of 20 μm. In order to calculate the stress intensity factor (SIF) the crack is presumed to be perpendicular to the surface below that point. The fact that the first part of the kinked crack (*a* in Figure 3) is very different from 90º will not affect the calculation of the SIF in the second part (*b* in Figure 3), even for high values of *a/b* (10> *a/b*) [12].

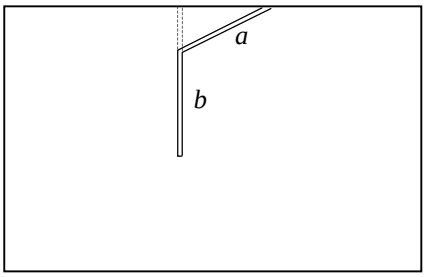

Figure 3: Kinked crack

There is mixed mode loading at the crack tip, but only K_I is going to be used because the crack is nearly perpendicular to the surface, and in this case mode II stress intensity factors are small compared to mode I, therefore the crack growth will not be significantly changed [2].

In order to calculate the SIF in mode I for a crack perpendicular to the surface, the following weight function calculated for an edge through crack in a two dimensional problem has been used [13].

$$w(t) = \frac{1}{\sqrt{t}}\left(1 + m_1 \cdot \frac{t}{a} + m_2 \cdot \left(\frac{t}{a}\right)^2\right) \tag{5}$$

where a, t and W are shown in Figure 4 and m_1 and m_2 are functions which depend on the ratio a/W. Using this weight function the stress intensity factor can be obtained from the expression:

$$K_I = \frac{\sqrt{2}}{\pi} \int_0^a w(t) \cdot \sigma_x(t)\, dt \tag{6}$$

where σ_x is the normal stress in the direction perpendicular to the crack plane. This stress intensity factor calculated has to be corrected to take into account the shape of the crack and that it is a three dimensional problem. The aspect ratio of the crack is approximately 0.5 and this gives a correction factor of 0.78, [14].

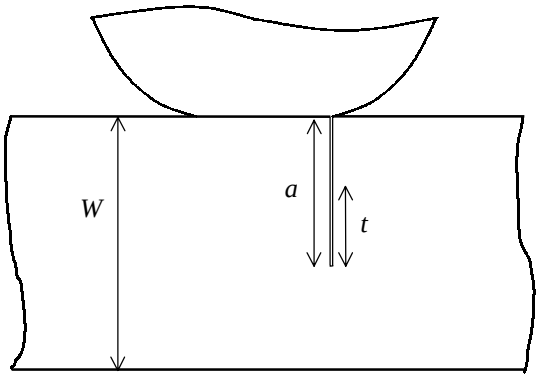

Figure 4: Cross section of the specimen

At this point different laws of propagation can be used. The data for crack growth in NASA/FLAGRO program [15] for Al 7075-T6 was chosen. This data coincides with other sources for long cracks [16,17] but not for short cracks where there is crack growth below the long crack threshold. The function used in the NASA/FLAGRO program, Eqn. 7. includes the effect of the stress ratio, *R*, the critical stress intensity factor, K_c, and the threshold stress intensity factor range, ΔK_{th}. This threshold can be corrected to include the small crack effect multiplying by a factor which depend on the crack length Eqn. 8. and Eqn. 9., [18].

$$\frac{da}{dN} = \frac{5.3465(1-R)^{-2.84}\Delta K^{2.836}(\Delta K - (1-R)\Delta K_{th}(a))^{0.5}}{((1-R)K_c - \Delta K)^{0.5}} \tag{7}$$

$$\Delta K_{th}(a) = \Delta K_{th\infty} \cdot \sqrt{\frac{a}{a+d}} \tag{8}$$

$$d = \frac{1}{\pi}\left(\frac{\Delta K_{th\infty}}{\Delta \sigma_f}\right)^2 \tag{9}$$

where *a* is the crack length, $\Delta K_{th\infty}$ is the threshold stress intensity factor range for long cracks and a stress ratio of *R*=0 and $\Delta\sigma_f$ is the fatigue limit. But this correction can be still insufficient. Figure 5 shows the propagation rate versus the stress intensity factor range for four different models. The first one is directly NASA/FLAGRO, and the second is NASA/FLAGRO corrected for short cracks using Eqn. 8. and Eqn. 9. The third is simply the Paris law, Eqn. 10, for this material for *R*=-1 and the data from [15], and the fourth is a curve obtained by Lankford [19] for Al 7075-T6 from different sources for short cracks. Actually this curve is the limit for short cracks with high stress levels. With lower stresses this curve would present a local minimum in the short crack region and the depth of it will depend, among other factors, on the stress level. Therefore, using this data to calculate the crack growth would give shorter lives. The four curves coincide for $\Delta K > 8$ Mpa $m^{1/2}$, that is long cracks, but below that value they are very different.

$$\frac{da}{dN} = 4.2151 \cdot 10^{-12}\ \Delta K^{3.517} \tag{10}$$

RESULTS

The results are summarized in Table 3. This table shows the crack initiation length, a_i, the initiation life, N_i, the propagation life, N_p, the total estimated life, N_T, and the experimental life, N_f.

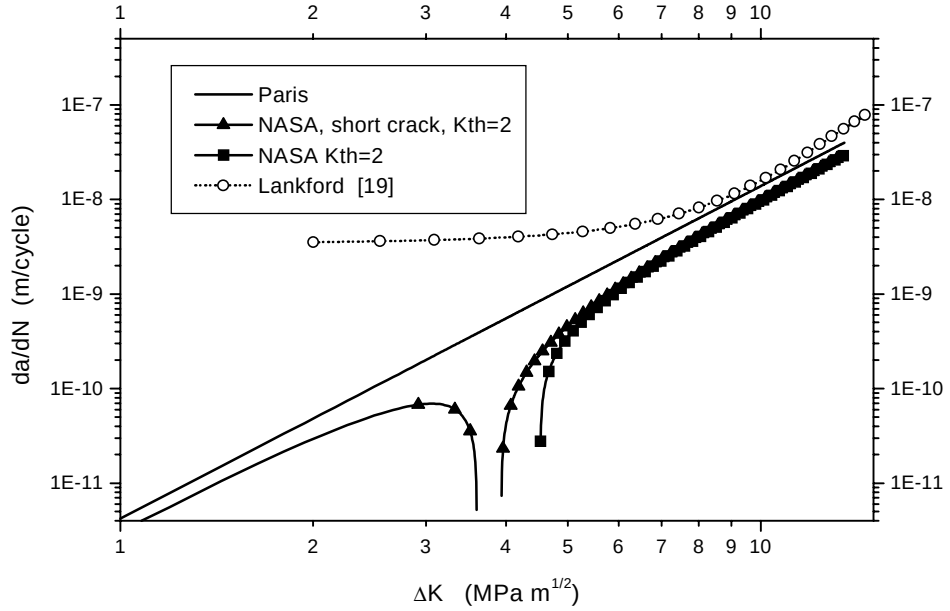

Figure 5: Different crack growth laws

TABLE 3
ESTIMATED LIVES AND CRACK INITIATION LENGTHS

Test	a_i (μm)	N_i	N_p	N_T	N_f
T1	26.6	133650	1948200	2081850	480000
T2	29.1	108127	1721692	1829819	449500
T3	34	94112	1394552	1488664	395000
T4	27.4	130075	2192140	2322215	551000
T5	27.5	145859	2096760	2242619	530000
T6	25.67	169606	2370520	2540126	803000
T7	28.6	215880	2392625	2608505	616500

McDiarmid multiaxial fatigue criterion was used in this paper, but any other could be used. As can be seen in Table 3, the life spent in initiation is considerably smaller than in propagation, so at this stage of the model and with these stress levels, other multiaxial fatigue criteria would have given similar results in the total estimated life. This means that for those stress levels more attention has to be paid to the propagation process. The crack initiation length calculated, 25-34 μm long, is longer than the depth at which the crack turns (about 20 μm), this means that stage I of the crack, where it grows at small angles, is included in the initiation process.

The crack growth law finally used to estimate the propagation life was the Paris law. The total estimated lives are shown in Figure 6, together with the estimated lives using the curve of Lankford shown in Figure 5 for four of the tests. The four tests chosen were the ones with the longest and shortest lives and two others in between. Real lives lie in the middle and this is because the crack growth rates shown in Figure 5 don't

represent the behavior for short cracks correctly. The Paris law does not show the behavior of short cracks and give too low crack growth rates and Lankford shows what seems to be the limit for short cracks and give too high rates. Lankford would be closer to reality for higher stresses (shorter lives), as can be seen in Figure 6. Using the correlation given by NASA/FLAGRO would give longer lives than Paris or it would predict that the crack did not grow, therefore it has not been included in the calculations.

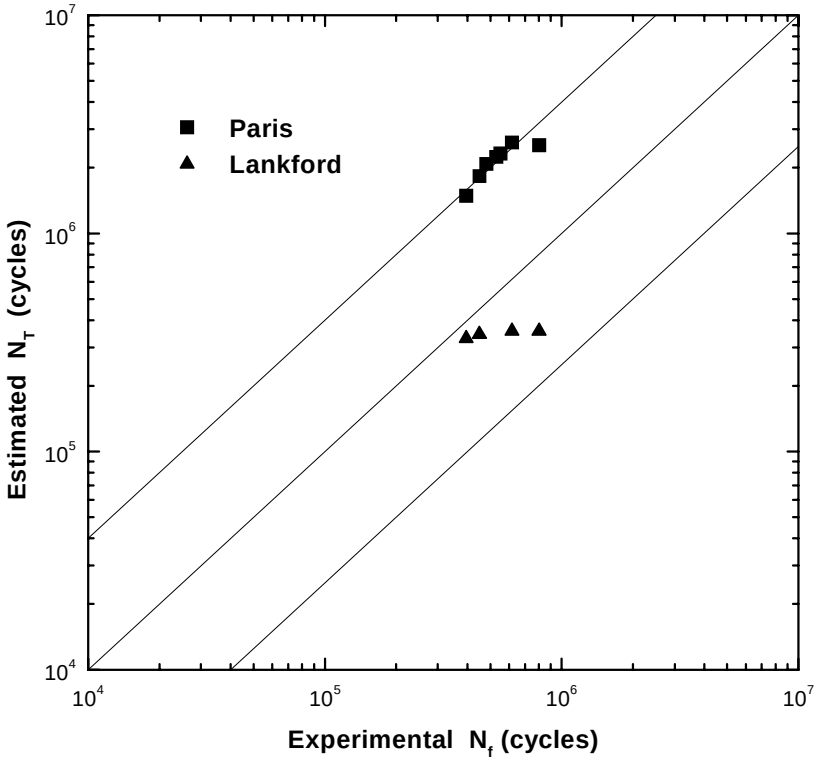

Figure 6: Estimated lives

CONCLUSIONS

An estimated life for a specimen subjected to fretting fatigue with spherical contact has been obtained considering the crack initiation and propagation, together with a non-arbitrary crack length. It has been shown that for the cases analyzed the initiation of the crack takes place very soon compared to the total life and that it includes the early stage of the crack where it grows at small angles.

The comparison of these estimates with the results of a series of tests, shows that the life is overestimated by a constant factor of 4 in the range of stresses studied when Paris crack growth law is considered. Closer values to reality are obtained using the law given by Lankford. This law is an upper bond for crack growth rate (lower bond for life estimate), therefore the lives obtained are underestimated. But, in this case there is not a constant factor in the error committed in the estimation.

More attention has to be paid to the growth of short cracks in order to obtain better results for the fatigue life. These results would also improve if mixed mode crack growth were considered as well as the inclination of the crack in stage II and the exact point of initiation.

ACKNOWLEDGEMENTS

The authors wish to thank the Ministerio de Educación y Cultura for their financial support through the investigation project with reference PB97-0696-C02-01.

REFERENCES

1. Waterhouse, R. B. and Lindley, T. C. (1994) *ESIS Publication* 18. MEP, London.
2. Faanes, S. and Fernando, U.S. (1994) *ESIS Publication* **18**, 149.
3. Szolwinski, M.P. and Farris, T.N., (1998) *Wear* **221**, 24.
4. Wittkowsky, B.U., Birch, P.R., Domínguez, J, Suresh, S., (1999) *Fretting Fatigue: Current Technology and Practices, ASTM STP 1367*
5. Wittkowsky, B.U., Birch, P.R., Domínguez, J, Suresh, S., (1999) *Fatigue Fract. Engng. Mater. Struct.* **22**, 307.
6. Socie, D.F., Morrow, J. and Chen, W.C., (1979) *J. Eng. Frac. Mech.* **11**, 851.
7. Chen, W.C. and Lawrence, F.V., Jr., (1977) *Progress Report in Advisory Committee of Fracture Control Program, College of Engineering, University of Illinois.*
8. Hamilton, G.M. (1983), *Proc. Of the Institution of Mechanical Engineering* **197C**, 53.
9. Navarro, C. And Domínguez J. (1999), *Computational Methods in Contact Mechanics IV*, 453.
10. McDiarmid, D.L., (1994), *Fatigue Fract. Engng. Mater. Struct.* **17**, 1475.
11. Chen, W.C. (1979). PhD Thesis, University of Illinois at Urbana-Champaign, U.S.A.
12. Hills D.A., Kelly, P.A., Dai D.N. and Korsunsky A.M. (1996). *Solution of Crack Problems: The Distributed Dislocation Technique*. Kluwer Academic Publishers, Dordrecht.
13. Bueckner, H.J. (1973). In: *Methods of analysis and solutions of crack problems*, pp. 306-307, Sih, G.C. (Eds). Noordhoff International Publishing, Leyden.
14. Suresh, S. (1998). *Fatigue of Materials*. Cambridge University Press, Cambridge.
15. Fatigue Crack Growth Computer Program, NASA/FLAGRO, (1986), L.B. Johson Space Center, JSC-22267.
16. Fatigue and Fracture, (1996), ASM Handbook **19**.
17. Taylor D. and Jianchun L. (1993) *Sourcebook on fatigue crack propagation: thresholds and crack closure*. EMAS, London.
18. El Haddad, M.H., Topper T.H. and Smith K.N. (1979) *Engineering Fracture Mechanics* **11**, 573.
19. Lankford, J. (1982) *Fatigue Engng. Mater. Struct.* **5**, 233.